agronomy

Article

Humic Acid Enhances the Soil Amelioration Effect of Biochar on Saline–Alkali Soils in Cotton Fields

Xiao Wang [1,2], Jianli Ding [1,2,3,*], Jinjie Wang [1,2,*], Lijing Han [4], Jiao Tan [1,2], Jingming Liu [1,2] and Xiangyu Ge [1,2]

[1] College of Geography and Remote Sensing Sciences, Xinjiang University, Urumqi 830017, China; xw33042@stu.xju.edu.cn (X.W.)
[2] Xinjiang Key Laboratory of Oasis Ecology, Xinjiang University, Urumqi 830017, China
[3] Xinjiang Institute of Technology, Aksu 843100, China
[4] College of Geodesy and Geomatics, Shandong University of Science and Technology, Qingdao 266590, China
* Correspondence: dingjl@xju.edu.cn (J.D.); wangjj@xju.edu.cn (J.W.); Tel.: +86-135-7926-5967 (J.D.); +86-158-0991-0816 (J.W.)

Abstract

To address the severe challenge of soil salinization, effective soil amelioration methods are urgently needed; however, current research on the microbial mechanisms of the combined application of multiple amendments is insufficient. Therefore, this study aims to investigate the impacts of biochar combined with humic acid (HA) on the physicochemical properties and microbial community structure of saline–alkali soils by a field experiment. The results showed that the co-application treatments significantly improved soil physicochemical properties and increased bacterial community richness; specific effects depended on the biochar feedstock. Notably, the H-MBC treatment was the most effective in reducing soil electrical conductivity (EC) by 44.1%, while the H-SBC treatment most significantly increased soil water content by 80.3%. Stochastic processes influenced the assembly of microbial communities, particularly the co-application group, forming a more complex and stable microbial network. Furthermore, Spearman correlation and random forest analyses revealed EC, nitrate nitrogen, and available phosphorus as the primary variables affecting microbial communities. These findings support the potential of the combined application of biochar and HA for saline–alkali soil amelioration, as this strategy mitigates salt stress and increases nutrient availability, thereby reshaping microbial communities toward states conducive to ecological restoration.

Keywords: saline–alkali soil; biochar; humic acid; microbial community structure; random forest

check for updates

Academic Editor: Jiafa Luo

Received: 19 September 2025
Revised: 7 October 2025
Accepted: 15 October 2025
Published: 17 October 2025

Citation: Wang, X.; Ding, J.; Wang, J.; Han, L.; Tan, J.; Liu, J.; Ge, X. Humic Acid Enhances the Soil Amelioration Effect of Biochar on Saline–Alkali Soils in Cotton Fields. *Agronomy* **2025**, *15*, 2412. https://doi.org/10.3390/agronomy15102412

1. Introduction

More than 10% of agricultural soils worldwide are affected by salinization, posing a serious threat to the sustainability of agricultural production [1,2]. As a globally important economic crop, although cotton has a certain degree of salt tolerance [3], its growth and metabolic activities are still closely linked to the soil environment and are extremely sensitive to salinization [4,5]. China is a major cotton producer, accounting for about 15% of the world's total planting area, with its production primarily concentrated in the Xinjiang region [6]. However, the scarcity of freshwater resources in Xinjiang often necessitates the use of mildly saline water for irrigation [7]. This practice not only exacerbates soil salinization, leading to compaction and reduced water and nutrient retention in farmland [8], but also disrupts the soil's microbial structure [9]. High salt stress is recognized as the primary limiting factor for cotton growth in northwestern China [10]. Through mechanisms such as osmotic stress, nutrient imbalances, and specific ion toxicity [11,12], it impairs the physiological functions and overall growth of cotton, ultimately causing reduced yields. In light of this, exploring effective soil amendment techniques to counteract salt stress has become an urgent research priority.

The application of organic amendments is a promising strategy for soil remediation [13]. Among them, biochar (a porous, carbon-rich material produced from biomass pyrolysis) and humic acid (HA, a natural organic compound) have been shown to improve soil physicochemical properties, enhance nutrient retention, and stimulate crop growth [14–17]. Notably, these amendments also profoundly influence the soil microbial community—a key driver of soil ecosystem health and nutrient cycling [18,19]. Soil bacteria, fungi, and microbial biomass are influenced by various soil properties, particularly salinity [20,21]. Elevated soil salinity increases osmotic pressure, leading to cellular dehydration, cell membrane rupture, and subsequent cell death in microbes [22,23]. The application of organic amendments in saline–alkali soils can significantly alter soil salinity and the overall microenvironment [24], thereby determining the composition of dominant microbial communities. Organic amendments also promote favorable shifts in microbial community structure, enhancing the abundance of salt-tolerant microbial taxa [25]. For example, in the cotton fields of Northwest China, various fertilization strategies have improved soil physicochemical properties, thereby increasing the populations of antagonistic bacteria [26]. Furthermore, certain microorganisms, such as *Pseudomonas* spp. and *Bacillus* spp., mitigate the toxicity of salt stress in plants through metabolic processes, including the synthesis of organic acids and secretion of stress-related enzymes [27,28]. Other halophilic microorganisms can actively uptake free sodium ions during their growth and reproduction [29]. Soil microorganisms are vital for plant growth, as studies have shown that higher microbial diversity enhances the efficiency of litter decomposition, thus providing more essential nutrients for plants [30,31]. Therefore, soil microorganisms serve not only as crucial indicators of soil ecosystem health but also as essential elements for achieving ecological restoration and improving agricultural productivity.

Biochar has been extensively studied in other soil types (e.g., paddy, acidic, and heavy metal-contaminated soils), but its application in saline–alkali soils is less explored, and improper feedstock selection can even worsen soil conditions [32–34]. Furthermore, most studies have focused on either biochar or HA alone. Research on the synergistic effects of combining biochar from different feedstocks with HA is particularly scarce, especially concerning the underlying microbial mechanisms driving soil improvement. It remains unclear how this combination specifically reshapes the microbial community to mitigate salt stress.

Therefore, this study aims to investigate the effects of biochar prepared from different feedstocks, applied alone or in combination with HA, on the physicochemical properties and microbial community structure of saline–alkaline soil. We seek to address the following scientific questions: (1) Can various soil amendment strategies effectively reduce soil salinity and enhance nutrient accumulation? Does the efficacy of biochar amendments specifically vary depending on the feedstock used? (2) How does HA enhance the effects of biochar? What is its specific role in influencing the microbial community? (3) What are the key environmental factors driving the structure and function of the microbial community in these soils?

2. Materials and Methods

2.1. Site Description

The experiment site is located in the 103rd Regiment of Wujiaqu City, Xinjiang, China (44°31′48″ N, 87°25′48″ E), at an altitude of 429 m (Figure 1a). The region experiences temperate, continental, and arid climates. During the experimental year, the mean annual temperature was 8.0 °C, with an annual precipitation of approximately 99.8 mm. Figure 1b illustrates the daily variations in rainfall and temperature. The soil at the site is sandy loam, with the following physicochemical properties: pH of 8.36, electrical conductivity (EC) of 1075 µS cm^{-1}, water content (SWC) of 5.8%, total carbon (TC) content of 12.52 g kg^{-1}, total nitrogen (TN) of 0.62 g kg^{-1}, total phosphorus (TP) of 0.58 g kg^{-1}, nitrate nitrogen ($NO_3{}^-$-N) of 8.73 mg kg^{-1}, and available phosphorus (AP) of 26.81 mg kg^{-1}.

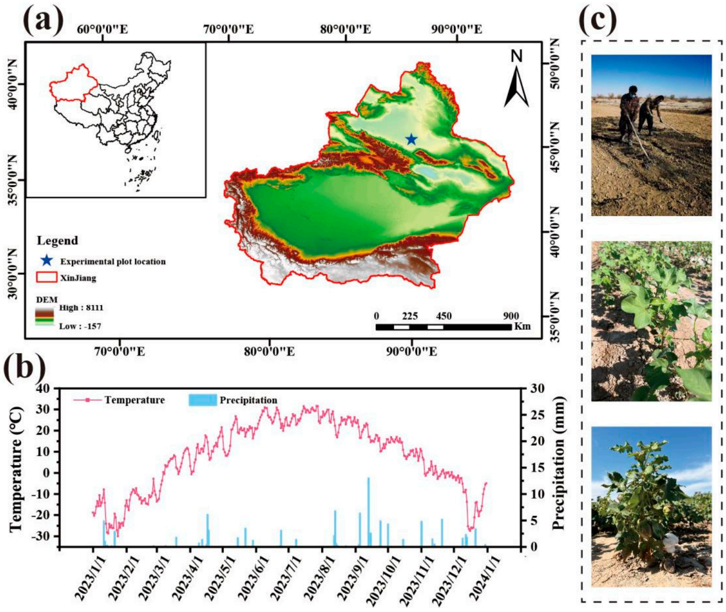

Figure 1. (**a**) Location of the experimental field; (**b**) precipitation and temperature data for 2023; (**c**) on-site photograph of the experimental plot.

2.2. Experimental Design and Soil Sampling

To investigate the effects of HA and different biochar feedstocks, this study was established as a two-factor factorial experiment arranged in a randomized block design. The two factors were HA (two levels: with and without) and biochar (three levels: no biochar, walnut shell biochar, and livestock manure biochar), resulting in the following six treatments:

(1) CK: Control (no amendment);
(2) HUM: HA only (0.6 t ha^{-1});
(3) SBC: Walnut shell biochar only (12 t ha^{-1});
(4) MBC: Livestock manure biochar only (12 t ha^{-1});
(5) H-SBC: Co-application of HA and walnut shell biochar (0.6 t ha^{-1} + 12 t ha^{-1});
(6) H-MBC: Co-application of HA and livestock manure biochar (0.6 t ha^{-1} + 12 t ha^{-1}).

Each treatment was replicated three times, for a total of 18 plots. Each plot measured 4 m × 4 m, with a minimum of 2 m spacing between plots to minimize cross-treatment interference. Biochar and HA were applied uniformly in a single application to the soil surface in early April 2023, followed by thorough mixing to a depth of 15–20 cm. The pyrolysis temperature of the biochars was between 400 °C and 500 °C.

The selected cotton variety, “Gengye 64,” was sown on 26 April 2023, with a planting density of 14,000 plants per 666.67 m^2. A wide–narrow row planting system with a single plastic film, two drip irrigation lines, and six rows (row spacing of 66 cm and 10 cm). Fertilization and other agronomic practices were consistent with conventional local field protocols.

Soil samples (0–20 cm depth) were collected on 14 September 2023. In each plot, five subsamples were randomly collected and combined to form one composite sample, resulting in a total of 18 independent composite samples for analysis. After removing plant roots and stones, each composite sample was homogenized and divided into two portions: one fresh portion for soil microbial analysis, and the other for determining soil physicochemical properties after air-drying.

2.3. Sample Analysis

The soil physicochemical indicators were determined following the procedures described by Bao [35].

High-throughput sequencing was used to analyze the soil microbial communities. Soil DNA extraction and high-throughput sequencing were performed by Shanghai Majorbio Bio-Pharm Technology Co., Ltd. (Shanghai, China) The specific steps were as follows: total DNA from the soil microbial community was extracted, and the quality of the extracted genomic DNA was accessed using 1% agarose gel electrophoresis. The bacterial 16S rDNA sequence was amplified using the primers 341F (5′-CCTAYGGGRBGCASCAG-3′) and 806R (5′-GGACTACNNGGGTATCTAAT-3′) on an ABI GeneAmp® 9700 PCR system (Applied Biosystems, Foster City, CA, USA) [36]. The amplified DNA fragments were purified through gel extraction, followed by library preparation, quantification, and quality control. High-throughput 16S rRNA sequencing was conducted on the Illumina MiSeq platform (Illumina, San Diego, CA, USA). The paired-end reads obtained from sequencing were assembled, quality-controlled, and filtered based on sequence overlapping to produce optimized sequences. Operational taxonomic units (OTUs) were clustered at a 97% similarity threshold using the USEARCH11-uparse algorithm.

2.4. Statistical Analysis

All statistical analyses were conducted using R version 4.3.1. Prior to analysis, data were assessed for the assumptions of normality using the Shapiro–Wilk test and for homogeneity of variances using Levene’s test. A two-way analysis of variance (ANOVA) was used to test the effects of the biochar amendment factor (B; no biochar, walnut shell biochar, livestock manure biochar), the humic acid factor (H; with or without humic acid), and their interaction (B × H) on soil physicochemical properties (EC, SWC, pH, TC, TP, TN, AP, NO_3^--N) and microbial α-diversity indices. When significant effects were detected by ANOVA, Duncan’s multiple range test was performed for post hoc comparisons. The statistical significance level was set at $p < 0.05$. Statistically significant differences are indicated by different lowercase letters in figures, and error bars represent the standard deviation (SD, $n = 3$).

To systematically elucidate the microbial community assembly processes in the biochar treatment group (BCs, including MBC and SBC) and the biochar combined with humic acid treatment group (HBCs, including H-MBC and H-SBC), we first calculated the modified stochasticity ratio (MST) using the NST package [37]. An MST value > 0.5 indicates that stochastic processes predominantly govern community assembly dynamics. In addition, we employed the neutral community model (NCM) proposed by Sloan et al. [38], in combination with the stats4, minpack.lm, and Hmisc packages, to further evaluate the role of stochasticity in the assembly of bacterial communities in both the BCs and HBCs groups.

Finally, the relative importance of deterministic processes, including homogeneous selection (HoS), heterogeneous selection (HeS), and stochastic processes, including homogenizing dispersal (HD), dispersal limitation (DL), and ecological drift (DR) in bacterial community assembly was quantified using the iCAMP framework (the Infer Community Assembly Mechanisms by Phylogenetic-bin-based null model) developed by Ning et al. [39].

Phylum-level taxa with a relative abundance > 0.05% and occurring in at least four samples were selected for co-occurrence analysis. Spearman's rank correlation coefficients were calculated, and only statistically significant associations ($|r| > 0.6$, $p < 0.05$) were retained. Co-occurrence networks were then constructed using the igraph package and visualized with Gephi (version 0.10). Furthermore, we analyzed the phylum-level taxonomic composition of nodes within the co-occurrence networks to identify key phyla that exhibited significant differences in relative abundance between the BCs and HBCs treatment groups. Specifically, intergroup differences were assessed using the Wilcoxon rank-sum test, with multiple testing correction performed using the Benjamini–Hochberg method. Confidence intervals (CIs) were estimated using the bootstrap method, and the results were visualized as extended error bar plots. The abundances of these key phyla were subsequently used as representative indicators to characterize the taxonomic composition of microbial co-occurrence networks.

To assess the influence of environmental factors on species community structure and to address the issue of multicollinearity, this study employed a Principal Component Analysis (PCA) dimensionality reduction strategy. We first performed PCA on the standardized environmental factors and selected the top N Principal Component scores (PC scores) as the RDA's explanatory variables, based on a cumulative variance contribution threshold greater than 90%. Subsequently, an RDA model was constructed using the Hellinger-transformed species data and these PC scores. The overall significance of the RDA model, as well as the significance of each constrained axis, was assessed using a permutation test with 999 permutations. Finally, the envfit function was utilized to fit the original environmental factors onto the RDA ordination plot, thereby identifying key factors with a significant driving effect ($p < 0.05$) on community structure. Based on this, the top 15 most abundant bacterial phyla were selected, and Spearman's rank correlation analysis was conducted in combination with key soil factors. A correlation heatmap was generated to visualize these associations.

Concurrently, to further assess the relative importance of key soil environmental variables in shaping the microbial co-occurrence networks, a random forest model was constructed within a 3-fold cross-validation framework repeated 20 times. Within each training fold, permutation importance (%IncMSE) was calculated based on out-of-bag (OOB) samples, and the selection frequency of the top 4 variables was used as a stability metric. A stability threshold of 60% (higher than the random selection probability of $4/8 = 50\%$) was set to identify the stable, important variables. Finally, a comprehensive ranking based on the average rank was conducted to screen for the most critical and stable driving factors.

3. Results

3.1. Response of Soil Physicochemical Properties

The application of biochar or HA improved the physicochemical properties of the saline–alkali soil (Figure 2). However, the combined application of biochar and HA yielded better results than their individual applications, and the specific effects varied depending on the biochar feedstock. Two-way ANOVA indicated a significant interaction effect between the biochar and HA factors in influencing key soil physicochemical properties ($B \times H$, $p < 0.05$). Specifically, compared to the CK, the H-MBC treatment was most effective in reducing soil EC by 44.1% and increasing AP by 45.8%; meanwhile, the H-SBC treatment was most prominent in increasing SWC by 80.3% and NO_3^--N by 44.5%. Furthermore, none of the treatments had a significant effect on soil pH.

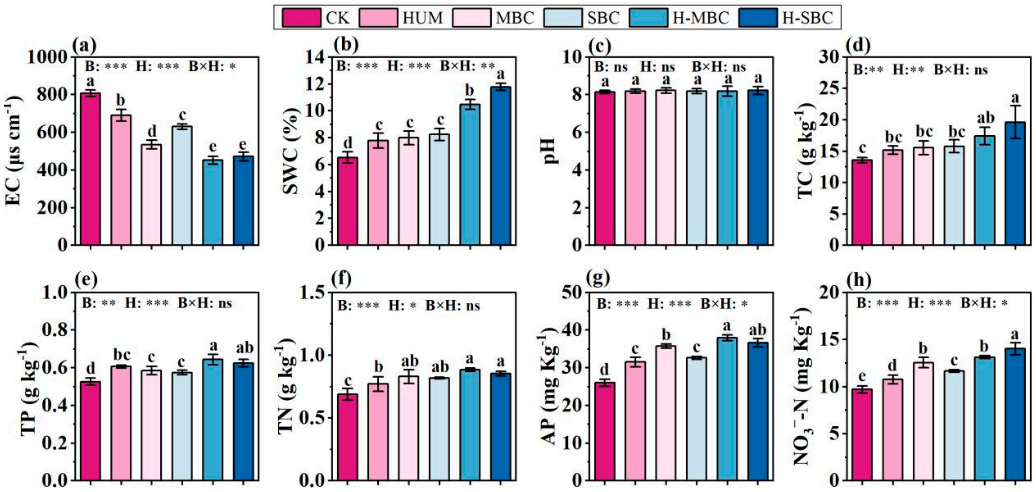

Figure 2. Soil physicochemical characteristics under different treatments. (**a**) electrical conductivity (EC); (**b**) water content (SWC); (**c**) pH; (**d**) total carbon (TC); (**e**) total phosphorus (TP); (**f**) total Nitrogen (TN); (**g**) available phosphorus (AP); (**h**) nitrate nitrogen (NO_3^--N). Error bars represent the standard deviation ($n = 3$). Different lowercase letters above the bars indicate significant differences among treatments at the $p < 0.05$ level. The symbols ns, *, **, and *** indicate no significant difference, and significant differences at the $p < 0.05$, $p < 0.01$, and $p < 0.001$ levels, respectively.

3.2. Changes in Bacterial Community Diversity and Taxa Composition

The bacterial richness indices were assessed, and the results showed that compared with the CK, sole biochar application significantly increased the ACE and Chao1 indices by 12.9–22.4% and 12.3–20.2%, respectively, while the combined application with HA led to increases of 17.2–27.4% and 15.9–26.0%. No significant differences were observed in the Simpson and Shannon indices among treatments (Figure 3a–d). NMDS results showed that the bacterial communities in soils subjected to different treatments formed distinctly separated clusters (Figure 3e). A two-way ANOVA revealed that the biochar amendment factor, the HA factor, and their interaction significantly affected soil microbial diversity (Figure 3a,b).

Bacterial phyla with a relative abundance > 0.5% were considered dominant. This study identified 11 dominant bacterial phyla that collectively comprised over 90% of the total bacterial community (Figure 4a). However, differences in bacterial taxa were observed across the various treatments. Compared to the CK, the application of biochar or HA alone significantly increased *Actinobacteriota* by 17.1–26.2%, while *Proteobacteria* and *Firmicutes* showed the opposite trend. Additionally, compared to the MBC treatment, the H-MBC treatment significantly reduced *Actinobacteriota* and *Chloroflexi* by 14.5% and 20.0%, respectively, while it significantly increased *Proteobacteria* by 32.1%. Two-way ANOVA revealed a significant interaction effect between biochar and HA on *Actinobacteriota*, *Proteobacteria*, *Firmicutes*, and *Chloroflexi* (Figure 4b).

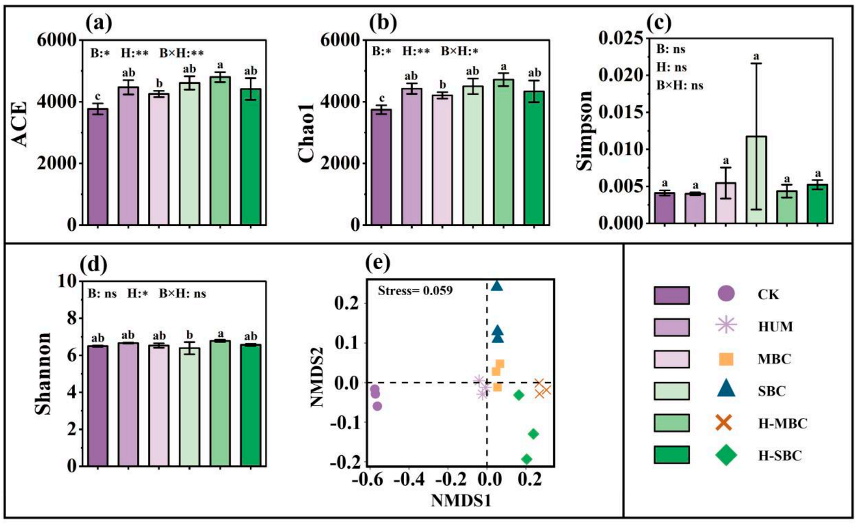

Figure 3. (**a**–**d**) Soil α-diversity indices of the bacterial community, including ACE, Chao1 index, Simpson index, and Shannon index. (**e**) β-diversity of soil bacterial communities based on non-metric multidimensional scaling (NMDS) analysis. The error bars represent the standard deviation ($n = 3$). Different lowercase letters above the bars indicate significant differences among treatments at the $p < 0.05$ level. The symbols ns, *, and ** indicate no significant difference, and significant differ-ences at the $p < 0.05$, and $p < 0.01$ levels, respectively.

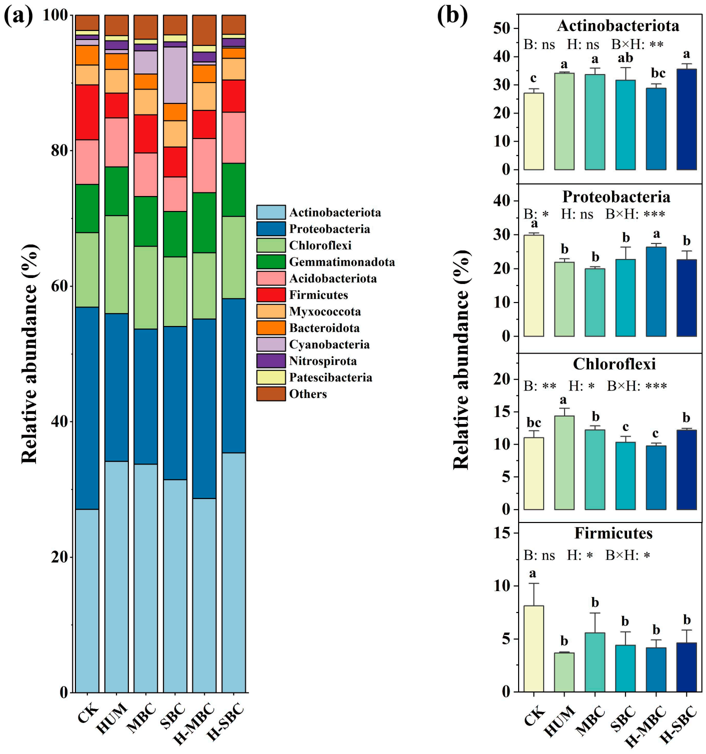

Figure 4. (**a**) Relative abundance composition of bacterial phyla for each treatment. (**b**) Bar plots of four representative phyla (*Actinobacteriota*, *Proteobacteria*, *Chloroflexi*, and *Firmicutes*), presented as mean ± standard deviation with error bars ($n = 3$). Different lowercase letters above the bars indicate significant differences among treatments at the $p < 0.05$ level. The symbols ns, *, **, and *** indicate no significant difference, and significant differ-ences at the $p < 0.05$, $p < 0.01$, and $p < 0.001$ levels, respectively.

3.3. Characteristics of Bacterial Community Assembly Processes

As mentioned above, the application of biochar in the presence of HA led to significant changes in the bacterial community structure. To further compare the different effects of biochar alone and in combination with HA on the bacterial community assembly process, the MST, NCM, and iCAMP methods were employed. The SBC and MBC treatments were categorized as the BCs group, while the H-SBC and H-MBC treatments were classified as the HBCs group. As shown in Figure 5a,b, the MST analysis indicated that the MST values for both groups were greater than 0.5, and the NCM model also showed a high goodness of fit, collectively confirming that stochastic processes were dominant in community assembly. Notably, the NCM analysis also found that the migration rate of the HBCs group (m = 0.867) was lower than that of the BCs group (m = 0.941), suggesting that the addition of HA to biochar reduced bacterial taxa dispersal, possibly leading to a more robust local community structure. Furthermore, iCAMP analysis quantified the role of ecological processes, revealing that stochastic processes had a larger contribution in the HBCs (93.8%) compared to the BCs group (90.4%), primarily driven by increased DR and DL. In summary, HA plays a crucial regulatory part in the biochar-soil interaction system by enhancing the dominance of stochastic processes, thereby shaping the assembly patterns of the community.

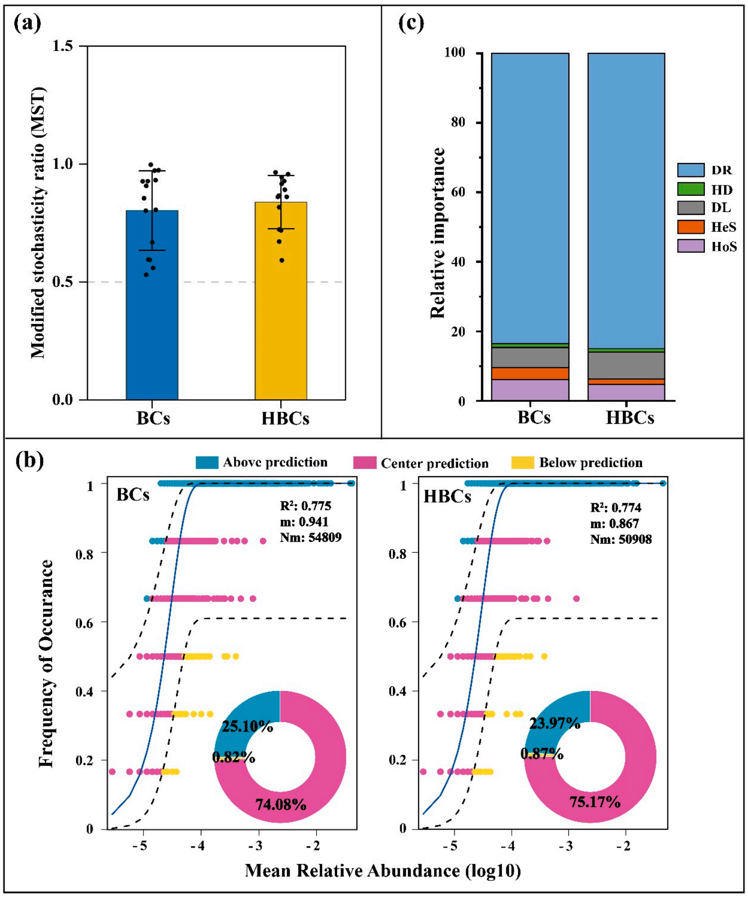

Figure 5. Soil bacterial community assembly processes in the biochar treatments group (BCs) and the combined biochar and humic acid treatments group (HBCs): (**a**) normalized stochasticity ratio (MST); (**b**) neutral community model (NCM); (**c**) infer community assembly mechanisms by phylogenetic-bin-based null model (iCAMP). The error bars represent the standard deviation.

3.4. Characteristics of the Bacterial Co-Occurrence Network and Keystone Taxa

To assess the impact of biochar and HA on the complexity and stability of the bacterial community, we constructed microbial co-occurrence networks. The results showed that, compared to the BCs group, the HBCs group formed a more complex and stable microbial network (Figure 6a). Specifically, the network of the HBCs group had more nodes (1410) and edges (1856), and the proportion of positive correlations (68.4%) was significantly higher than that of the BCs group (55.5%). Therefore, the synergistic effect of biochar and HA likely optimized the coexistence patterns of microorganisms, enhancing the stability and functional redundancy of the entire community by constructing a complex network dominated by positive cooperation.

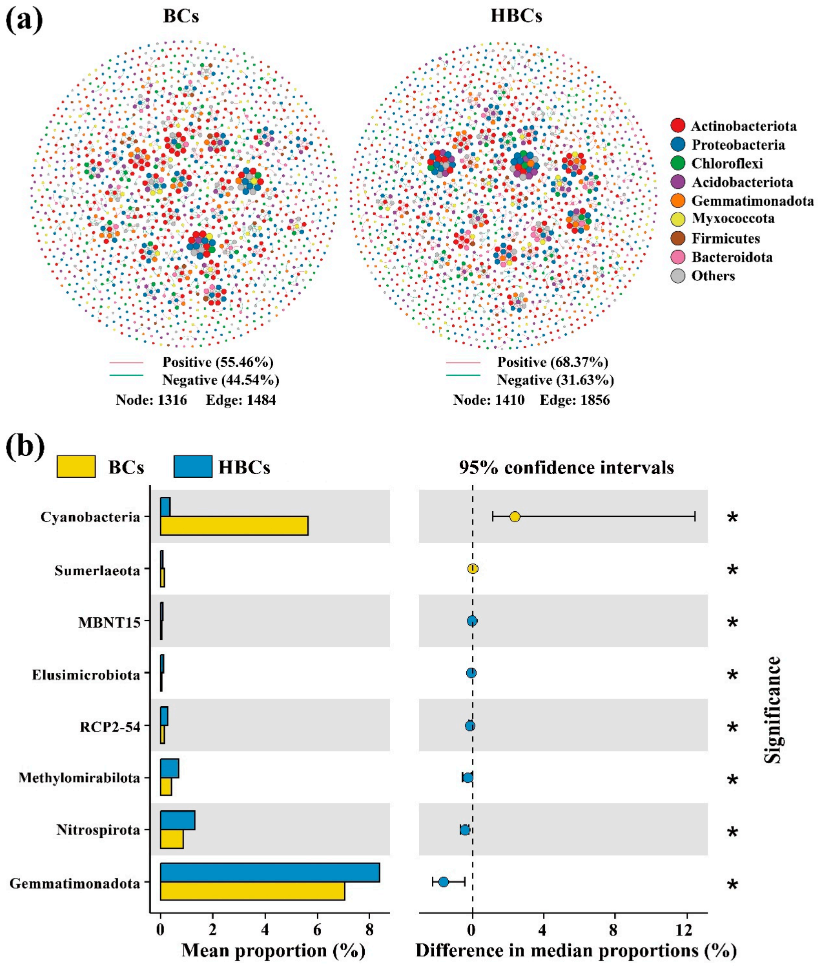

Figure 6. (**a**) Microbial co-occurrence network patterns in the biochar treatments group (BCs) and the combined biochar and humic acid treatments group (HBCs); (**b**) extended error bar plot illustrating the effects of BCs and HBCs on the relative abundance of bacterial phyla showing significant differences. Asterisks indicate significance levels (*: $p < 0.05$).

To further identify the key species contributing to the differences in the microbial community network characteristics between the BCs and HBCs groups, an extended error bar plot was used to display the significantly different taxa (Figure 6b). The results showed that eight bacterial taxa exhibited significant differences when HA was treated as a random factor. The addition of HA significantly increased the abundance of *Gemmatimonadota*, *Nitrospirota*, *Methylomirabilota*, *RCP2-54*, *Elusimicrobiota*, and *MBNT15*, with *Gemmatimonadota* showing the most significant increase. In contrast, *Cyanobacteria* levels significantly decreased. These changes in bacterial taxa were the primary contributors to the differences in the co-occurrence networks between the BCs and HBCs groups.

3.5. Key Environmental Drivers of the Bacterial Community

To determine the crucial environmental factors influencing the shifts in the microbial community, we conducted an RDA. The results suggested that application strategies led to significant differentiation in the microbial community structure, with soil physicochemical properties being the main variables explaining this variation (explaining 38.5%) (Figure 7a).

To further explore the relationship between these soil factors and the abundance of major bacterial phyla, we performed a Spearman correlation analysis (Figure 7b). This analysis revealed that soil EC was a crucial factor, showing significant negative correlations with the abundance of several major phyla, such as *Methylomirabilota*, *Gemmatimonadota*, *Armatimonadota*, and *Nitrospirota*. Conversely, the availability of key nutrients (especially NO_3^--N and AP) was positively correlated with these phyla. In addition, the Random Forest model analysis (Figure 8) results showed that EC, NO_3^--N, and AP were the most critical soil factors influencing the compositional features of the bacterial co-occurrence network. In summary, these results indicate that soil salinity and nutrient status are the primary environmental factors mediating the impacts of the specific application strategies on the bacterial community.

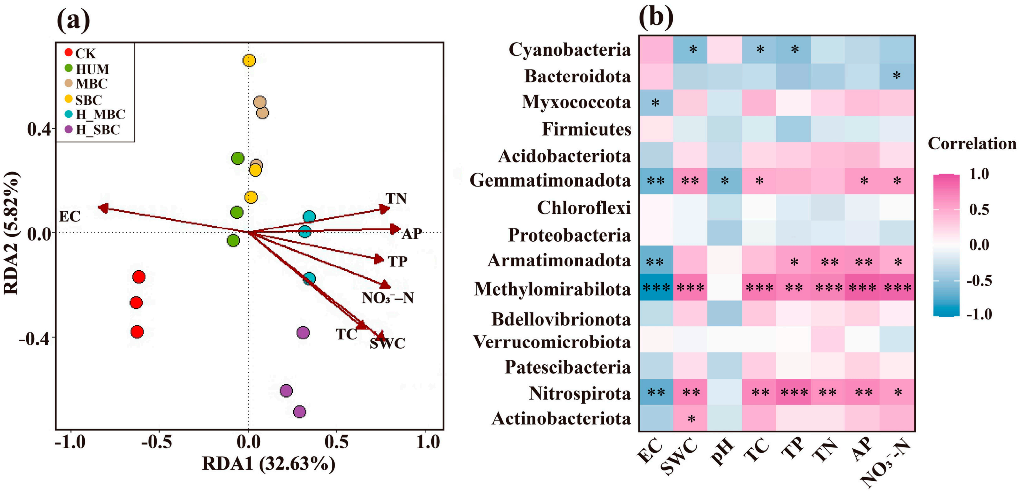

Figure 7. (**a**) Redundancy analysis (RDA) ordination plot of the soil microbial community and soil physicochemical properties. Sample points are colored according to their treatment groups, and red arrows indicate the environmental variables that are significantly correlated with the ordination axes. The first two constrained axes are displayed; the overall model and the first axis were significant as determined by 999 permutation tests (overall model: $p < 0.001$; RDA1: $p < 0.001$; RDA2: $p = 0.275$). (**b**) Spearman's rank correlation heatmap of the relationship between soil physicochemical properties and the top 15 dominant bacterial phyla. The color intensity represents the strength of the correlation, and asterisks indicate the significance levels (*: $p < 0.05$, **: $p < 0.01$, ***: $p < 0.001$).

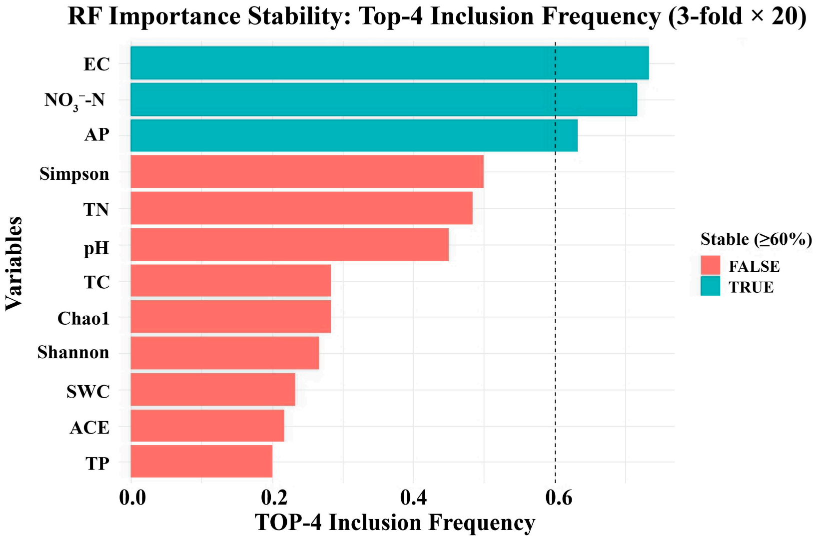

Figure 8. Random forest importance stability (top-4 inclusion frequency).

4. Discussion

4.1. Effect of Biochar from Different Feedstock Combined with Humic Acid on Soil Properties

The combined application of biochar and HA is an effective strategy for enhancing soil fertility and remediating saline–alkali soils. This study found that the combined treatment decreased soil EC by up to 44.1% and significantly increased nutrient content by 45.8%, an efficacy far exceeding that of single amendments. By comparison, the effects of single amendments reported in the literature are relatively limited. For instance, a meta-analysis by Li et al. [40] indicated that conventional organic materials decreased soil EC by an average of 23.6%, while Wang et al. [41] reported that the application of inorganic amendments resulted in a 26.8% reduction. This superior performance is attributed to the synergistic effects of biochar and HA at the physical, chemical, and biological levels [42]. Physically, the combination of biochar's porous structure and the cementing ability of HA significantly optimized soil aggregate structure, enhancing the soil's aeration, water permeability, and capacity for water and nutrient retention [43,44]. Chemically, the combined active functional groups and adsorption sites from both materials substantially increased the soil's cation exchange capacity, improving nutrient adsorption and slow-release [45,46]. Simultaneously, the chelating effect of HA activated immobilized micronutrients, and together, they enhanced overall nutrient availability [47,48]. Biologically, this composite amendment provided habitats and nutrient sources for soil microorganisms, thereby stimulating microbial activity and fostering a healthier micro-ecological environment [49].

However, the efficacy of the synergistic improvement is not constant; the key factor lies in the feedstock used for biochar production [50]. For instance, wood-based biochar has a greater advantage in improving soil physical structure [51,52], whereas biochar derived from livestock manure is not only rich in readily available nutrients, but the Ca^{2+} and Mg^{2+} released during its mineralization can also effectively displace exchangeable Na^+ [53,54]. This is also corroborated by our research findings: the combination of manure biochar and HA was significantly superior to that of walnut shell biochar in reducing salinity and increasing nutrients. Therefore, the key to achieving the optimal remediation effect lies in scientifically selecting the biochar feedstock based on the specific problems of the target soil (e.g., poor structure, salinization, or nutrient deficiency) and combining it with HA in a rational proportion. Future applications will require a more precise matching of biochar type, soil conditions, and crop requirements to achieve sustainable increases in agricultural productivity.

4.2. Regulatory Mechanisms of Soil Amendment Strategies on Microbial Ecological Processes and Co-Occurrence Networks

This study found that, compared to the sole application of biochar, the combined application of biochar and HA significantly enhanced the complexity of the soil bacterial co-occurrence network. We attribute this reshaping of the network structure to synergistic regulatory mechanisms at two distinct levels. First, by optimizing soil physicochemical properties, the combined application provided a direct driving force and a biological foundation for the complexification of the microbial network [55]. On one hand, biochar and HA significantly enhanced soil fertility, creating favorable conditions for microbial cooperation. Nutrient-rich environments can promote the formation of microbial aggregates or biofilms for more efficient resource utilization, thereby increasing material exchange and information transfer and fostering closer interactions [56,57]. On the other hand, the improved soil environment also supported higher bacterial diversity. Higher species diversity implies a greater variety of ecological niches and potential functional complementarities, laying the species foundation for a more complex co-occurrence network [58–60]. The study by Lu et al. [61] also confirmed that composite amendments are superior to single amendments in enhancing both microbial diversity and network complexity.

At a deeper level, this increase in network complexity is rooted in a fundamental shift in the microbial community assembly process. Microbial community assembly is a critical nexus linking the environment to network structure [62,63]. Under saline–alkali stress, deterministic processes driven by environmental filtering typically predominate [64,65]. However, our study revealed that the combined application of biochar and HA significantly enhanced the contribution of stochastic processes to community assembly (Figure 5), a finding consistent with reports by Wang et al. [66] on the effects of organic amendments. This shift from deterministic to stochastic processes is crucial because when the pressure from environmental filtering is alleviated (i.e., soil conditions improve), the stochastic processes (such as DL and DR processes) become more significant [67–69]. These stochastic processes give rise to greater diversity and heterogeneity in microbial interactions, thus fundamentally driving the increase in network complexity [70].

4.3. Mechanisms of Soil Salinity and Nutrient Supply on Microbial Communities

Soil EC, NO_3^--N, and AP as the most critical predictors driving variations in the microbial community structure (Figure 8). Soil salinity, as the primary abiotic stress factor, constitutes a strong environmental filter for community assembly [71,72]; whereas after the alleviation of salt stress, nutrient availability becomes the key determinant of community differentiation and functional divergence [73]. The strong filtering effect of EC is primarily manifested in its holistic selection pressure on the microbial community [74]. High salinity directly affects microbial osmotic regulation and enzyme activity [75], thereby leading to a general suppression of community diversity and selecting for specific taxa possessing high salt-tolerance capabilities [76]. The high responsiveness of the phylum *Methylomirabilota* to EC fluctuations observed in our study is a direct manifestation of this selection mechanism; the abundance of this group was strongly suppressed under high-salinity conditions, but after salt stress was mitigated by co-application, it exhibited strong competitive adaptability to the low-salinity, high-nutrient environment.

Therefore, the core ecological mechanism of this co-application strategy can be summarized as a reshaping of the hierarchical influence of environmental drivers. By reducing EC, these measures weakened the dominant role of abiotic stress (environmental filtering) in community assembly, thereby allowing biological processes, such as resource competition and niche partitioning, to become the key determining factors in shaping the community structure [77,78]. For example, the increase in nitrate nitrogen provided a competitive advantage for known microorganisms involved in the nitrogen cycle (e.g., *Methylomirabilota*). Meanwhile, the increased availability of phosphorus, a key limiting element for microbial growth [79], generally promoted microbial metabolic activities and community abundance [80,81]. This shift in driving forces—from being dominated by environmental filtering to being dominated by resource competition—is the fundamental reason for the recovery of the soil microbial community from a stressed state and the re-establishment of more active biogeochemical processes, such as the nitrogen cycle, which are governed by key functional guilds [82,83].

4.4. Limitations and Implications

This study provides high-reliability field evidence for the synergistic effects of co-applying biochar and HA in the management of saline–alkali soils, particularly for cotton cultivation, which significantly enhances the practical value of the findings. Compared to traditional soil amelioration measures such as high-intensity leaching, frequent application of gypsum, or the sole use of inorganic fertilizers, the co-application strategy demonstrates lower management costs and labor requirements, while offering more significant soil improvement effects [84,85]. However, although the raw material for biochar is low-cost, its production and transportation costs remain a potential economic barrier to large-scale adoption. Therefore, a comprehensive life-cycle assessment is required in the future to quantify its long-term sustainability. Concurrently, the limitations of this study include its short-term nature (a single growing season) and single-site characteristic, which restrict conclusions on the long-term stability and broad-spectrum applicability of the amendments' effects. Future research should focus on conducting multi-year field trials and incorporating molecular tools like metagenomics to further elucidate the biogeochemical mechanisms that drive the improvement of soil functions, thereby providing more precise and economically viable field management recommendations for cotton growers.

5. Conclusions

Our research systematically evaluated the effects of biochar and its co-application with HA on the physicochemical properties, bacterial community structure, and ecological assembly processes of saline–alkali soil. We confirmed that this co-application strategy exhibits a significant synergistic effect and is biochar feedstock-dependent in saline–alkali soil reclamation. Specifically, H-MBC demonstrated the best performance in reducing soil EC and increasing AP, while H-SBC showed outstanding advantages in improving soil SWC and increasing NO_3^--N. At the level of microbial ecology, the combined use of biochar and HA not only significantly enhanced community richness but also constructed a complex, tightly connected co-occurrence network dominated by positive cooperation by strengthening the prevalence of stochastic assembly processes. Further analysis identified EC, NO_3^--N, and AP as the core environmental factors mediating the impact of the co-application strategy on bacterial community structure. In summary, this co-application strategy effectively drove the microbial community, making it more favorable for ecological restoration by alleviating salt stress and improving nutrient availability. Therefore, we suggest that agricultural managers adopt the combined application of biochar and HA as an alternative to traditional amendments, based on specific reclamation goals, to simultaneously enhance soil quality and support crop growth in arid saline environments.

Author Contributions: Methodology, X.W. and J.W.; Software, L.H.; Formal analysis, J.T.; Writing—original draft, X.W.; Writing—review & editing, J.D.; Supervision, J.W., J.L. and X.G.; Project administration, J.W.; Funding acquisition, J.D. All authors have read and agreed to the published version of the manuscript.

Funding: This research was funded by the Technology Innovation Team (Tianshan Innovation Team), the Innovative Team for Efficient Utilization of Water Resources in Arid Regions (NO. 2022TSYCTD0001), and the Key Project of Natural Science Foundation of Xinjiang Uygur Autonomous Region (No. 2021D01D06).

Data Availability Statement: Dataset available on request from the authors: The raw data supporting the conclusions of this article will be made available by the authors on request.

Conflicts of Interest: The authors declare no conflict of interest.

References

1. Zaman, M.; Shahid, S.A.; Heng, L.; Shahid, S.A.; Zaman, M.; Heng, L. Soil salinity: Historical perspectives and a world overview of the problem. In *Guideline for Salinity Assessment, Mitigation and Adaptation Using Nuclear and Related Techniques*; Springer: Cham, Switherland, 2018; pp. 43–53.
2. Xiong, J.; Ge, X.; Ding, J.; Wang, J.; Zhang, Z.; Zhu, C.; Han, L.; Wang, J. Optimal time-window for assessing soil salinity via Sentinel-2 multitemporal synthetic data in the arid agricultural regions of China. *Ecol. Indic.* **2025**, *176*, 113642. [CrossRef]

3. Khan, M.A.; Wahid, A.; Ahmad, M.; Tahir, M.T.; Ahmed, M.; Ahmad, S.; Hasanuzzaman, M. World cotton production and consumption: An overview. In *Cotton Production and Uses: Agronomy, Crop Protection, and Postharvest Technologies*; Springer: Singapore, 2020; pp. 1–7.
4. Zhang, H.; Li, D.; Zhou, Z.; Zahoor, R.; Chen, B.; Meng, Y. Soil water and salt affect cotton (*Gossypium hirsutum* L.) photosynthesis, yield and fiber quality in coastal saline soil. *Agric. Water Manag.* **2017**, *187*, 112–121. [CrossRef]
5. Ashraf, M. Salt tolerance of cotton: Some new advances. *Crit. Rev. Plant Sci.* **2002**, *21*, 1–30. [CrossRef]
6. Dai, J.; Dong, H. Intensive cotton farming technologies in China: Achievements, challenges and countermeasures. *Field Crops Res.* **2014**, *155*, 99–110. [CrossRef]
7. Yang, G.; Li, F.; Tian, L.; He, X.; Gao, Y.; Wang, Z.; Ren, F. Soil physicochemical properties and cotton (*Gossypium hirsutum* L.) yield under brackish water mulched drip irrigation. *Soil Tillage Res.* **2020**, *199*, 104592. [CrossRef]
8. Paranychianakis, N.; Chartzoulakis, K. Irrigation of Mediterranean crops with saline water: From physiology to management practices. *Agric. Ecosyst. Environ.* **2005**, *106*, 171–187. [CrossRef]
9. Chen, L.; Li, C.; Feng, Q.; Wei, Y.; Zhao, Y.; Zhu, M.; Deo, R.C. Direct and indirect impacts of ionic components of saline water on irrigated soil chemical and microbial processes. *Catena* **2019**, *172*, 581–589. [CrossRef]
10. Xiao, C.; Ji, Q.; Zhang, F.; Li, Y.; Fan, J.; Hou, X.; Yan, F.; Liu, X.; Gong, K. Effects of various soil water potential thresholds for drip irrigation on soil salinity, seed cotton yield and water productivity of cotton in northwest China. *Agric. Water Manag.* **2023**, *279*, 108172. [CrossRef]
11. Sharif, I.; Aleem, S.; Farooq, J.; Rizwan, M.; Younas, A.; Sarwar, G.; Chohan, S.M. Salinity stress in cotton: Effects, mechanism of tolerance and its management strategies. *Physiol. Mol. Biol. Plants* **2019**, *25*, 807–820. [CrossRef] [PubMed]
12. Shahid, M.A.; Sarkhosh, A.; Khan, N.; Balal, R.M.; Ali, S.; Rossi, L.; Gómez, C.; Mattson, N.; Nasim, W.; Garcia-Sanchez, F. Insights into the physiological and biochemical impacts of salt stress on plant growth and development. *Agronomy* **2020**, *10*, 938. [CrossRef]
13. Yupeng, W.; Yufei, L.; Yanmeng, B.; Zhenjun, S. Responses of saline soil properties and cotton growth to different organic amendments. *Pedosphere* **2018**, *28*, 521–529. [CrossRef]
14. El-Sayed, M.E.; Hazman, M.; Abd El-Rady, A.G.; Almas, L.; McFarland, M.; Shams El Din, A.; Burian, S. Biochar reduces the adverse effect of saline water on soil properties and wheat production profitability. *Agriculture* **2021**, *11*, 1112. [CrossRef]
15. Kul, R.; Arjumend, T.; Ekinci, M.; Yildirim, E.; Turan, M.; Argin, S. Biochar as an organic soil conditioner for mitigating salinity stress in tomato. *Soil Sci. Plant Nutr.* **2021**, *67*, 693–706. [CrossRef]
16. Ampong, K.; Thilakaranthna, M.S.; Gorim, L.Y. Understanding the role of humic acids on crop performance and soil health. *Front. Agron.* **2022**, *4*, 848621. [CrossRef]
17. Tahoun, A.M.A.; El-Enin, M.M.A.; Mancy, A.G.; Sheta, M.H.; Shaaban, A. Integrative soil application of humic acid and foliar plant growth stimulants improves soil properties and wheat yield and quality in nutrient-poor sandy soil of a semiarid region. *J. Soil Sci. Plant Nutr.* **2022**, *22*, 2857–2871. [CrossRef]
18. Singh Rawat, V.; Kaur, J.; Bhagwat, S.; Arora Pandit, M.; Dogra Rawat, C. Deploying microbes as drivers and indicators in ecological restoration. *Restor. Ecol.* **2023**, *31*, e13688. [CrossRef]
19. Philippot, L.; Chenu, C.; Kappler, A.; Rillig, M.C.; Fierer, N. The interplay between microbial communities and soil properties. *Nat. Rev. Microbiol.* **2024**, *22*, 226–239. [CrossRef] [PubMed]
20. Canfora, L.; Salvati, L.; Benedetti, A.; Francaviglia, R. Is soil microbial diversity affected by soil and groundwater salinity? Evidences from a coastal system in central Italy. *Environ. Monit. Assess.* **2017**, *189*, 319. [CrossRef]
21. Rath, K.M.; Murphy, D.N.; Rousk, J. The microbial community size, structure, and process rates along natural gradients of soil salinity. *Soil Biol. Biochem.* **2019**, *138*, 107607. [CrossRef]
22. Hou, Y.; Zeng, W.; Hou, M.; Wang, Z.; Luo, Y.; Lei, G.; Zhou, B.; Huang, J. Responses of the soil microbial community to salinity stress in maize fields. *Biology* **2021**, *10*, 1114. [CrossRef]
23. Shah, G.; Jan, M.; Afreen, M.; Anees, M.; Rehman, S.; Daud, M.; Malook, I.; Jamil, M. Halophilic bacteria mediated phytoremediation of salt-affected soils cultivated with rice. *J. Geochem. Explor.* **2017**, *174*, 59–65. [CrossRef]
24. Mao, T.; Wang, Y.; Ning, S.; Mao, J.; Sheng, J.; Jiang, P. Assessment of the effects of biochar on the physicochemical properties of saline–alkali soil based on meta-analysis. *Agronomy* **2024**, *14*, 2431. [CrossRef]
25. Mao, X.; Yang, Y.; Guan, P.; Geng, L.; Ma, L.; Di, H.; Liu, W.; Li, B. Remediation of organic amendments on soil salinization: Focusing on the relationship between soil salts and microbial communities. *Ecotoxicol. Environ. Saf.* **2022**, *239*, 113616. [CrossRef]
26. Li, R.; Tao, R.; Ling, N.; Chu, G. Chemical, organic and bio-fertilizer management practices effect on soil physicochemical property and antagonistic bacteria abundance of a cotton field: Implications for soil biological quality. *Soil Tillage Res.* **2017**, *167*, 30–38. [CrossRef]
27. Naz, I.; Bano, A. Biochemical, molecular characterization and growth promoting effects of phosphate solubilizing *Pseudomonas* sp. isolated from weeds grown in salt range of Pakistan. *Plant Soil* **2010**, *334*, 199–207. [CrossRef]

28. Hasanuzzaman, M.; Raihan, M.R.H.; Nowroz, F.; Fujita, M. Insight into the mechanism of salt-induced oxidative stress tolerance in soybean by the application of Bacillus subtilis: Coordinated actions of osmoregulation, ion homeostasis, antioxidant defense, and methylglyoxal detoxification. *Antioxidants* **2022**, *11*, 1856. [CrossRef] [PubMed]
29. Oren, A. Diversity of halophilic microorganisms: Environments, phylogeny, physiology, and applications. *J. Ind. Microbiol. Biotechnol.* **2002**, *28*, 56–63. [CrossRef]
30. Giller, K.E.; Cadisch, G. Driven by Nature: A Sense of Arrival and Departure. In *Driven by Nature: Plant Litter Quality and Decomposition*; Cadisch, G., Giller, K.E., Eds.; CAB International: Wallingford, UK, 1997; pp. 393–399.
31. Chiba, A.; Uchida, Y.; Kublik, S.; Vestergaard, G.; Buegger, F.; Schloter, M.; Schulz, S. Soil bacterial diversity is positively correlated with decomposition rates during early phases of maize litter decomposition. *Microorganisms* **2021**, *9*, 357. [CrossRef]
32. Wu, M.; Feng, Q.; Sun, X.; Wang, H.; Gielen, G.; Wu, W. Rice (*Oryza sativa* L) plantation affects the stability of biochar in paddy soil. *Sci. Rep.* **2015**, *5*, 10001. [CrossRef]
33. Rechberger, M.V.; Kloss, S.; Rennhofer, H.; Tintner, J.; Watzinger, A.; Soja, G.; Lichtenegger, H.; Zehetner, F. Changes in biochar physical and chemical properties: Accelerated biochar aging in an acidic soil. *Carbon* **2017**, *115*, 209–219. [CrossRef]
34. He, L.; Zhong, H.; Liu, G.; Dai, Z.; Brookes, P.C.; Xu, J. Remediation of heavy metal contaminated soils by biochar: Mechanisms, potential risks and applications in China. *Environ. Pollut.* **2019**, *252*, 846–855. [CrossRef]
35. Bao, S. *Soil and Agricultural Chemistry Analysis*; China Agricultural Press: Beijing, China, 2000.
36. Behrendt, L.; Larkum, A.W.; Trampe, E.; Norman, A.; Sørensen, S.J.; Kühl, M. Microbial diversity of biofilm communities in microniches associated with the didemnid ascidian Lissoclinum patella. *ISME J.* **2012**, *6*, 1222–1237. [CrossRef]
37. Ning, D.; Deng, Y.; Tiedje, J.M.; Zhou, J. A general framework for quantitatively assessing ecological stochasticity. *Proc. Natl. Acad. Sci. USA* **2019**, *116*, 16892–16898. [CrossRef] [PubMed]
38. Sloan, W.T.; Lunn, M.; Woodcock, S.; Head, I.M.; Nee, S.; Curtis, T.P. Quantifying the roles of immigration and chance in shaping prokaryote community structure. *Environ. Microbiol.* **2006**, *8*, 732–740. [CrossRef] [PubMed]
39. Ning, D.; Yuan, M.; Wu, L.; Zhang, Y.; Guo, X.; Zhou, X.; Yang, Y.; Arkin, A.P.; Firestone, M.K.; Zhou, J. A quantitative framework reveals ecological drivers of grassland microbial community assembly in response to warming. *Nat. Commun.* **2020**, *11*, 4717. [CrossRef]
40. Li, T.; Wang, S.; Liu, S.; Zhang, X.; Dong, H.; Dai, S.; Chai, L.; Li, H.; Lv, Y.; Li, T. Trade-offs of organic amendment input on soil quality and crop productivity in saline-alkali land globally: A meta-analysis. *Eur. J. Agron.* **2025**, *164*, 127471. [CrossRef]
41. Wang, X.; Ding, J.; Wang, J.; Han, L.; Tan, J.; Ge, X. Ameliorating saline-sodic soils: A global meta-analysis of field studies on the influence of exogenous amendments on crop yield. *Land Degrad. Dev.* **2024**, *35*, 3330–3343. [CrossRef]
42. Malik, Z.; Malik, N.; Noor, I.; Kamran, M.; Parveen, A.; Ali, M.; Sabir, F.; Elansary, H.O.; El-Abedin, T.K.Z.; Mahmoud, E.A. Combined effect of rice-straw biochar and humic acid on growth, antioxidative capacity, and ion uptake in maize (*Zea mays* L.) grown under saline soil conditions. *J. Plant Growth Regul.* **2023**, *42*, 3211–3228. [CrossRef]
43. Hammerschmiedt, T.; Holatko, J.; Pecina, V.; Huska, D.; Latal, O.; Kintl, A.; Radziemska, M.; Muhammad, S.; Gusiatin, Z.M.; Kolackova, M. Assessing the potential of biochar aged by humic substances to enhance plant growth and soil biological activity. *Chem. Biol. Technol. Agric.* **2021**, *8*, 46.
44. Hasanuzzaman, M.; Nowroz, F.; Raihan, M.R.H.; Siddika, A.; Alam, M.M.; Prasad, P.V. Application of biochar and humic acid improves the physiological and biochemical processes of rice (*Oryza sativa* L.) in conferring plant tolerance to arsenic-induced oxidative stress. *Environ. Sci. Pollut. Res.* **2024**, *31*, 1562–1575. [CrossRef]
45. Singh, C.; Tiwari, S.; Gupta, V.K.; Singh, J.S. The effect of rice husk biochar on soil nutrient status, microbial biomass and paddy productivity of nutrient poor agriculture soils. *Catena* **2018**, *171*, 485–493. [CrossRef]
46. Lehmann, J.; Rillig, M.C.; Thies, J.; Masiello, C.A.; Hockaday, W.C.; Crowley, D. Biochar effects on soil biota–a review. *Soil Biol. Biochem.* **2011**, *43*, 1812–1836. [CrossRef]
47. Ni, H.; Zhao, J.; Yang, Z. Effects of compound fertilizer decrement and water-soluble humic acid fertilizer application on soil properties, bacterial community structure, and shoot yield in Lei Bamboo (Phyllostachys praecox) plantations in subtropical China. *Forests* **2024**, *15*, 400. [CrossRef]
48. Guo, Y.; Ma, Z.; Ren, B.; Zhao, B.; Liu, P.; Zhang, J. Effects of humic acid added to controlled-release fertilizer on summer maize yield, nitrogen use efficiency and greenhouse gas emission. *Agriculture* **2022**, *12*, 448. [CrossRef]
49. Zhang, Y.; Miao, S.; Song, Y.; Wang, X.; Jin, F.J.S. Biochar application reduces saline–alkali stress by improving soil functions and regulating the diversity and abundance of soil bacterial community in highly saline–alkali paddy field. *Sustainability* **2024**, *16*, 1001. [CrossRef]
50. Gabhane, J.W.; Bhange, V.P.; Patil, P.D.; Bankar, S.T.; Kumar, S. Recent trends in biochar production methods and its application as a soil health conditioner: A review. *SN Applied Sciences* **2020**, *2*, 1307. [CrossRef]
51. Yao, T.; Zhang, W.; Gulaqa, A.; Cui, Y.; Zhou, Y.; Weng, W.; Wang, X.; Liu, Q.; Jin, F.; Nutrition, P. Effects of peanut shell biochar on soil nutrients, soil enzyme activity, and rice yield in heavily saline-sodic paddy field. *J. Soil Sci. Plant Nutr.* **2021**, *21*, 655–664. [CrossRef]

52. Sun, J.; He, F.; Shao, H.; Zhang, Z.; Xu, G. Effects of biochar application on Suaeda salsa growth and saline soil properties. *Environ. Earth Sci.* **2016**, *75*, 630. [CrossRef]
53. Dahlawi, S.; Naeem, A.; Rengel, Z.; Naidu, R. Biochar application for the remediation of salt-affected soils: Challenges and opportunities. *Sci. Total. Environ.* **2018**, *625*, 320–335. [CrossRef]
54. Wang, X.; Ding, J.; Han, L.; Tan, J.; Ge, X.; Nan, Q.J.G. Biochar addition reduces salinity in salt-affected soils with no impact on soil pH: A meta-analysis. *Geoderma* **2024**, *443*, 116845. [CrossRef]
55. Van Der Heijden, M.G.; Bardgett, R.D.; Van Straalen, N.M. The unseen majority: Soil microbes as drivers of plant diversity and productivity in terrestrial ecosystems. *Ecol. Lett.* **2008**, *11*, 296–310. [CrossRef] [PubMed]
56. Solanki, M.K.; Solanki, A.C.; Kumari, B.; Kashyap, B.K.; Singh, R.K. Plant and soil-associated biofilm-forming bacteria: Their role in green agriculture. In *New and Future Developments in Microbial Biotechnology and Bioengineering: Microbial Biofilms*; Elsevier: Amsterdam, The Netherlands, 2020; pp. 151–164.
57. Joseph, S.; Cowie, A.L.; Van Zwieten, L.; Bolan, N.; Budai, A.; Buss, W.; Cayuela, M.L.; Graber, E.R.; Ippolito, J.A.; Kuzyakov, Y. How biochar works, and when it doesn't: A review of mechanisms controlling soil and plant responses to biochar. *Gcb Bioenergy* **2021**, *13*, 1731–1764. [CrossRef]
58. Wu, B.; Ding, M.; Zhang, H.; Devlin, A.T.; Wang, P.; Chen, L.; Zhang, Y.; Xia, Y.; Wen, J.; Liu, L. Reduced soil multifunctionality and microbial network complexity in degraded and revegetated alpine meadows. *J. Environ. Manag.* **2023**, *343*, 118182. [CrossRef]
59. Shen, H.; Wang, B.; Jiao, Y.; Zhang, X.; Zhang, Q.; Xiong, Z. Bacteria are more sensitive than fungi to soil fertility in an intensive vegetable field. *Appl. Soil Ecol.* **2023**, *190*, 105003. [CrossRef]
60. Shu, X.; He, J.; Zhou, Z.; Xia, L.; Hu, Y.; Zhang, Y.; Zhang, Y.; Luo, Y.; Chu, H.; Liu, W. Organic amendments enhance soil microbial diversity, microbial functionality and crop yields: A meta-analysis. *Sci. Total Environ.* **2022**, *829*, 154627. [CrossRef]
61. Lu, C.; Zhang, Z.; Guo, P.; Wang, R.; Liu, T.; Luo, J.; Hao, B.; Wang, Y.; Guo, W. Synergistic mechanisms of bioorganic fertilizer and AMF driving rhizosphere bacterial community to improve phytoremediation efficiency of multiple HMs-contaminated saline soil. *Sci. Total Environ.* **2023**, *883*, 163708. [CrossRef]
62. Sun, C.; Zhang, B.; Ning, D.; Zhang, Y.; Dai, T.; Wu, L.; Li, T.; Liu, W.; Zhou, J.; Wen, X. Seasonal dynamics of the microbial community in two full-scale wastewater treatment plants: Diversity, composition, phylogenetic group based assembly and co-occurrence pattern. *Water Res.* **2021**, *200*, 117295. [CrossRef] [PubMed]
63. Gralka, M.; Szabo, R.; Stocker, R.; Cordero, O.X. Trophic Interactions and the Drivers of Microbial Community Assembly. *Curr. Biol.* **2020**, *30*, R1176–R1188. [CrossRef] [PubMed]
64. Xu, Y.; Sun, R.; Yan, W.; Zhong, Y. Divergent response of soil microbes to environmental stress change under different plant communities in the Loess Plateau. *Catena* **2023**, *230*, 107240. [CrossRef]
65. Valverde, A.; Makhalanyane, T.P.; Cowan, D.A. Contrasting assembly processes in a bacterial metacommunity along a desiccation gradient. *Front. Microbiol.* **2014**, *5*, 668. [CrossRef]
66. Wang, Y.-X.; Liu, X.-Y.; Di, H.-H.; He, X.-S.; Sun, Y.; Xiang, S.; Huang, Z.-B. The mechanism of microbial community succession and microbial co-occurrence network in soil with compost application. *Sci. Total Environ.* **2024**, *906*, 167409. [CrossRef]
67. Xu, Z.; Sun, R.; He, T.; Sun, Y.; Wu, M.; Xue, Y.; Meng, F.; Wang, J. Disentangling the impact of straw incorporation on soil microbial communities: Enhanced network complexity and ecological stochasticity. *Sci. Total Environ.* **2023**, *863*, 160918.
68. Zhu, L.; Luan, L.; Chen, Y.; Wang, X.; Zhou, S.; Zou, W.; Han, X.; Duan, Y.; Zhu, B.; Li, Y. Community assembly of organisms regulates soil microbial functional potential through dual mechanisms. *Glob. Change Biol.* **2024**, *30*, e17160.
69. Nemergut, D.R.; Schmidt, S.K.; Fukami, T.; O'Neill, S.P.; Bilinski, T.M.; Stanish, L.F.; Knelman, J.E.; Darcy, J.L.; Lynch, R.C.; Wickey, P. Patterns and processes of microbial community assembly. *Microbiol. Mol. Biol. Rev.* **2013**, *77*, 342–356. [CrossRef]
70. Huo, X.; Ren, C.; Wang, D.; Wu, R.; Wang, Y.; Li, Z.; Huang, D.; Qi, H. Microbial community assembly and its influencing factors of secondary forests in Qinling Mountains. *Soil Biol. Biochem.* **2023**, *184*, 109075. [CrossRef]
71. Sritongon, N.; Sarin, P.; Theerakulpisut, P.; Riddech, N. The effect of salinity on soil chemical characteristics, enzyme activity and bacterial community composition in rice rhizospheres in Northeastern Thailand. *Sci. Rep.* **2022**, *12*, 20360. [CrossRef] [PubMed]
72. Yuan, B.-C.; Li, Z.-Z.; Liu, H.; Gao, M.; Zhang, Y.-Y. Microbial biomass and activity in salt affected soils under arid conditions. *Appl. Soil Ecol.* **2007**, *35*, 319–328. [CrossRef]
73. Chen, H.; Ma, K.; Huang, Y.; Fu, Q.; Qiu, Y.; Yao, Z. Significant response of microbial community to increased salinity across wetland ecosystems. *Geoderma* **2022**, *415*, 115778. [CrossRef]
74. Rath, K.M.; Maheshwari, A.; Rousk, J. Linking microbial community structure to trait distributions and functions using salinity as an environmental filter. *mbio* **2019**, *10*, e1607–e1619. [CrossRef]
75. Galinski, E.A.; Trüper, H.G. Microbial behaviour in salt-stressed ecosystems. *FEMS Microbiol. Rev.* **1994**, *15*, 95–108. [CrossRef]
76. Wang, X.; Xu, L.; Qi, X.; Huang, J.; Han, M.; Wang, C.; Li, X.; Jiang, H. Microbial assembly and stress-tolerance mechanisms in salt-adapted plants along the shore of a Salt Lake: Implications for saline–alkaline soil remediation. *Microorganisms* **2025**, *13*, 1942. [CrossRef]

77. Litchman, E.; Edwards, K.F.; Klausmeier, C.A. Microbial resource utilization traits and trade-offs: Implications for community structure, functioning, and biogeochemical impacts at present and in the future. *Front. Microbiol.* **2015**, *6*, 254. [CrossRef] [PubMed]
78. Dini-Andreote, F.; de Cássia Pereira e Silva, M.; Triado-Margarit, X.; Casamayor, E.O.; Van Elsas, J.D.; Salles, J.F. Dynamics of bacterial community succession in a salt marsh chronosequence: Evidences for temporal niche partitioning. *ISME J.* **2014**, *8*, 1989–2001. [CrossRef] [PubMed]
79. Menge, D.N.; Hedin, L.O.; Pacala, S.W. Nitrogen and phosphorus limitation over long-term ecosystem development in terrestrial ecosystems. *PLoS ONE* **2012**, *7*, e42045. [CrossRef]
80. Wu, W.; Wang, F.; Xia, A.; Zhang, Z.; Wang, Z.; Wang, K.; Dong, J.; Li, T.; Wu, Y.; Che, R. Meta-analysis of the impacts of phosphorus addition on soil microbes. *Agric. Ecosyst. Environ.* **2022**, *340*, 108180. [CrossRef]
81. Liu, L.; Gundersen, P.; Zhang, T.; Mo, J. Effects of phosphorus addition on soil microbial biomass and community composition in three forest types in tropical China. *Soil Biol. Biochem.* **2012**, *44*, 31–38. [CrossRef]
82. Neher, D. Soil community composition and ecosystem processes: Comparing agricultural ecosystems with natural ecosystems. *Agrofor. Syst.* **1999**, *45*, 159–185. [CrossRef]
83. Albornoz, F.E.; Prober, S.M.; Ryan, M.H.; Standish, R.J. Ecological interactions among microbial functional guilds in the plant-soil system and implications for ecosystem function. *Plant Soil* **2022**, *476*, 301–313. [CrossRef]
84. Li, G.; Shan, Y.; Bai, Y.; Nie, W.; Wang, Q.; Zhang, J.; Liu, H.; Ding, Y.; Wang, X.; Lu, H. Synergistic Effects of Humic Acid, Biochar-Based Microbial Agent, and Vermicompost on the Dry Sowing and Wet Emergence Technology of Cotton in Saline–Alkali Soils, Xinjiang, China. *Agronomy* **2024**, *14*, 994.
85. Zhao, W.; Xiao, J.; Wang, S.; Gai, X.; Chen, G. Bone biochar and humic acid improved soil quality and promoted Olea europaea growth in coastal saline soil by enhancing the stoichiometric homeostasis of nutrient elements. *Biochar* **2025**, *7*, 70. [CrossRef]